# Additive Manufacturing with Borosilicate Glass and Soda-Lime Glass


**F. Fröhlich, J. Hildebrand, and J. P. Bergmann**

**Abstract** In this paper, the possibility of additively producing individual 3D-structures with borosilicate and soda-lime glass based on a laser process with glass rods is demonstrated. In a previous study, process parameters, which show the geometrically defined deposition of individual layers were determined (Fröhlich et al. in Herstellung individueller Strukturen aus silikatischen Werkstoffen mittels Wire-Laser Additive Manufacturing. Wilhelm & Sohn, pp. 287–297, 2020). These findings are used to create single-layer walls, flat applications and free-form structures. The focus is on the additive manufacturing of large-volume components compared to the current state of the art. A $CO_2$ laser is used to create a melt pool on the substrate surface. The rod-based additional material is melted to create 3D-structures. The ratio between process speed and feed speed, as well as the laser power, remains constant during the experiments, as does the temperature in the process chamber. The fabricated structures are subjected to thermal post-treatment to reduce thermal stress. Remaining residual stresses are investigated with photoelasticity. The samples are quantified with destructive and non-destructive materialographical tests to determine the geometric dimensions. Taking into account the previous process parameters, the results achieved are discussed and evaluated with regard to the width, height of the layer and the bonding angle. The height adjustment in relation to the layer height is discussed in order to avoid shape deviation. The major objective of the investigation is to achieve near-net-shape production with a low tensile residual stress state in order to reduce the degree of post-processing.

**Keywords** Additive manufacturing · Glass · Borosilicate glass · Soda-lime glass · $CO_2$ laser

F. Fröhlich (✉) · J. Hildebrand · J. P. Bergmann
Production Technology Group, Technische Universität Ilmenau, Gustav-Kirchhoff-Platz, 98693 Ilmenau, Germany
e-mail: fabian.froehlich@tu-ilmenau.de

J. Hildebrand
e-mail: joerg.hildebrand@tu-ilmenau.de

J. P. Bergmann
e-mail: jeanpierre.bergmann@tu-ilmenau.de



L. F. M. da Silva et al. (eds.), *2nd International Conference on Advanced Joining Processes (AJP 2021)*, Proceedings in Engineering Mechanics,
https://doi.org/10.1007/978-3-030-95463-5_10

## 1 Introduction

Properties of glass, such as transparency, thermal linear expansion, chemical and thermal resistance, is increasingly used in additive manufacturing technologies this material. The different technologies open up new possibilities in the production of glass and functionalities of the resulting components, which are not technically possible with the previous technologies. The layer-by-layer construction of components gives the designer freedom in functionality and design, which is limited by the starting material and the additive manufacturing technology. Possible 3D-Printing technologies for glass are Selective Laser Sintering (SLS) (Klocke et al. 2004; Lee et al. 1995), Selective Laser Melting (SLM) (Fateri et al. 2014; Fateri and Gebhardt 2015; Kinzel et al. 2014; Khmyrov et al. 2014; Khmyrov et al. 2016), Fused Deposition Modeling (FDM) (Klein et al. 2016, 2012; Seel et al. 2018; Gal-Or et al. 2019), Stereolithography (SLA) (Kotz et al. 2017, 2016; Liu et al. 2018), Direct Ink Writing (Nguyen et al. 2017) and Direct Energy Deposition-Laser (DED-L) (Fröhlich et al. 2020; Kinzel et al. 2014; Luo et al. 2016, 2017, 2018; Witzendorff et al. 2018; Grabe et al. 2021).

However, glass has extremely high melting temperatures, non-linear thermo-mechanical properties of glass and is sensitive to thermal shocks (Schaeffer and Langfeld 2020). This poses different challenges for the additive manufacturing processes mentioned. In the SLS or SLM process, glass is typically fed as a powder material. During production, the laser moves over the powder bed layer by layer and scans the object contour. Depending on the possible packing density of the glass powder, cavities between the grains being fused during production and remaining in the component lead to defects similar to bubbles (Kinzel et al. 2014). If the density of the manufactured component is to be increased, it is subjected to thermal post-treatment. This subjects the component to shrinkage and consequently to geometric deviation (Klocke et al. 2004). Kinzel et al. (2014) shows the advantages of using solid material as compared to powder to manufacture optical components. In the AM technology SLA and Direct Ink Writing, a composite material containing glass powder is used as the starting material (Kotz et al. 2017, 2016; Nguyen et al. 2017). The production of a green body from the glass-containing composite material can be done at room temperature. To obtain a glassy body, the green body compact must be subjected to a long heat treatment process. During this process, the solvents and organic binders outgas from the green body. The outgassing requires volatile binders, which also limit the thickness of the wall structures produced (Gal-Or et al. 2019). However, these processes are suitable for small-scale objects with a high level of detail. This contrasts with FDM, where Klein et al. (2016) can achieve a print volume of 460 $mm^3/s$ according to the design. The average height of a layer was 4.5 mm and the width 9.5 mm with a contour deviation of 0.5 mm (Klein et al. 2016). A typical feature of the technology is the distinct layer structure, which creates a wavy surface. Because gravity is used to feed the molten glass from the crucible through the nozzle, a constant fill level is necessary here. The varying filling level had a negative effect on the printing result. It was observed that the glass stuck to the nozzle during printing

rather than to the colder previous printed layer (Klein et al. 2016). The wear that occurs on the crucible, i.e. the detachment of surface particles from the crucible wall by the molten glass, also has a negative effect on the printing result (Vogel 1993). In the DED-L technology, a melt is created on the sample surface of the glass with the energy carrier laser, into which the filler material is fed and melted (Fröhlich et al. 2020; Kinzel et al. 2014; Luo et al. 2016, 2017, 2018; Witzendorff et al. 2018; Grabe et al. 2021). For glass processing, the use of a $CO_2$ laser with a wavelength of 10.6 µm is typical, as glass is opaque in this range (Gräf et al. 2013). Defects caused by inhomogeneities due to powdery starting materials or particles of the technical periphery, stress cracks due to wall thicknesses and lack of opportunities for outgassing solvents and organic binders can be avoided for large-format components if solid material is used for additive manufacturing without intermediate steps. If fibres are used as filler material, they are covered with a polymer coating for better handling. The coating is removed mechanically in an additional step before feeding or melted off by the laser (Witzendorff et al. 2018; Grabe et al. 2021). However, there is a risk that particle residues can get into the melt. For optical elements, Luo et al. (2018) have shown that the use of glass rods achieves good results. If glass rods made of soda-lime glass are used, it is necessary to preheat the substrate with a hot plate in order to keep the thermal shock as low as possible (Luo et al. 2017). Due to the high thermal shock resistance of quartz glass, a heating plate for substrate preheating is not necessary (Luo et al. 2018; Grabe et al. 2021). Increasing the number of layers, the distance between the manufacturing point and the preheated substrate will be greater. Due to the poor thermal conductivity of glass, only the first layers are sufficiently preheated for manufacturing. From the point of lowering heat influence from the hot plate, the thermal gradient between the fabrication point and the base plate increases. This leads for glasses like soda lime and borosilicate glass to a greater susceptibility to cracking during the additive manufacturing process.

In this work, the possibility of additive manufactured individual 3D structures from borosilicate and soda-lime glass based on a laser process with glass rods is demonstrated. Knowledge from previous work is used to create single-layer walls, planar applications and individual structures. The focus is on the additive manufacturing of large-volume components compared to the current state of the art. In addition, an experimental setup will be created that can process several types of glass.

## 2 Experimental Setup and Preliminary Work

With the aim of developing a process that guarantees the additive manufacturing of individual structures made of glass, both in height and in planar area, the greatest potential was seen in the Direct Energy Deposition Laser (DED-L) process. A $CO_2$ laser is used to create a melt pool on the surface of the substrate. The rod-shaped additional material is fed and melted to create 3D structures (Fig. 1) (Fröhlich et al. 2020). The relative movement in the plane (X–Y) of the specimen to the working point is implemented by two linear tables offset by 90° in their direction of movement.

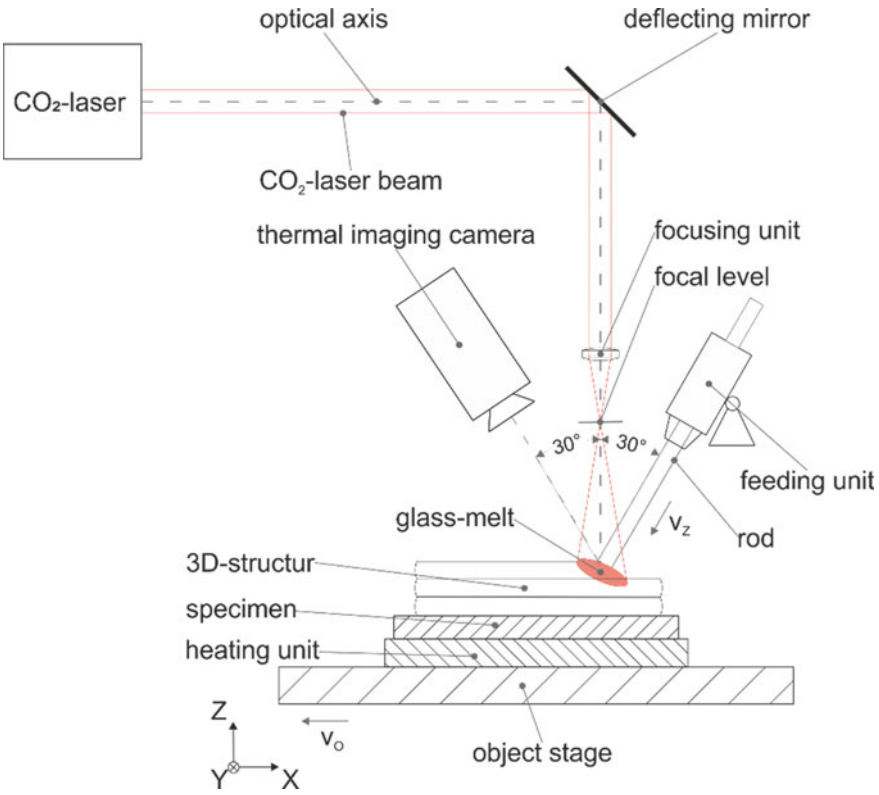


**Fig. 1** Sketch of the experimental setup of the Direct Energy Deposition Laser process (Fröhlich et al. 2020)

Geared DC motors with the SM 400 control move these. The shift of the working point in height is implemented by moving the focussing unit along the Z-axis. A heating plate is used to reduce the thermal gradient in the additive manufacturing of borosilicate and soda lime glass. The accessibility of the set-up enables the use of non-contact measuring methods. A thermal imaging camera (model MC320FHT) from the company LumaSense Technologies GmbH is used to monitor the temperatures generated in the process. The calibrated temperature range extends from 400 to 1800 °C. Maximum temperatures of up to 2100 °C can be measured. The measurement uncertainty according to the manufacturer is ± 2 K or 2% of the measured value. The thermal imaging camera is aligned at an angle of 30° to the laser beam and orthogonal to the direction of manufacturing. The reduction of the thermal gradient generated by the laser beam from the glass surface during additive manufacturing is implemented by the focusing unit method. A stronger defocusing of the laser beam increases the interaction range between the laser beam and the glass surface. The $CO_2$ laser beam source used (Synrad firestar f400, $\lambda = 10.6$ µm, continuous wave) is aligned perpendicular to the specimen. The majority of the area of the incident

laser beam diameter is used to heat the substrate. The calculated interaction diameter between laser and glass surface is approximately 10 mm. The distance between the focusing unit and the substrate surface was not changed during the experiments. The feeding unit is a proprietary development. A stepper motor constantly feeds the additional material into the melt at a speed of 1 mm/s via a linear rail. By means of a manual three-axis positioning system, the feed point of the additional material can be adjusted to the melt. The feed angle is adjusted by a turntable and remains constant during the tests at an angle of 30° between the feed axis and the $CO_2$ laser beam. The direction of feed and the direction of movement of the object table are in the same direction, which results in a dragging arrangement. Borofloat® and float glass from SCHOTT are used as specimens for the experiments. The dimensions of the specimens are 50 × 50 × 3 mm. The additional material used are glass rods made of Duran® (2 mm diameter) and AR-Glas® (3 mm diameter) from SCHOTT. It has been shown that the thermal gradient between the substrate and the working point grows with increasing component height. The working point moves further and further away from the zone of the sample that is thermally influenced by the hot plate. In order to avoid thermal fracture of the sample, the experimental setup is changed as shown in Fig. 2. Due to the oven bell, a measurement with non-contact measuring methods is now not possible. Therefore, the previous measurement results and findings are used to draw conclusions about the process inside the oven bell. A Synrad firestar f201 with $\lambda = 10.6\ \mu m$ in cw mode was used for the setup shown in Fig. 2. The heating plate was replaced by an oven bell. Inside the process chamber, a constant temperature of 500 °C was maintained during the experiments with a deviation of ± 15 K. The movement of the specimen inside the process chamber was realised with a three-axis system. Stepper motors drive the linear axes, which are controlled by a CNC card module. In this setup, the focusing unit is not moved, the constancy of the working point in the layer build-up is ensured by the z-axis of the object table. The feed direction for the experiments was perpendicular to the object table speed.

## 3 Results

The morphologies of the additively manufactured layers produced in the previous investigations (Fröhlich et al. 2020) confirm the results of Luo et al. (2017). By using rods with a diameter of 2 mm (borosilicate glass) and 3 mm (soda-lime glass), a higher laser power is necessary compared to Luo et al. (2017). The line energy for individual additively manufactured layers is calculated as follows (1):

$$E = \frac{P}{v_O} \tag{1}$$

The line energy refers to the laser power and the object table speed and has the unit J/mm. The ratio between the object table speed and the feed rate remains constant

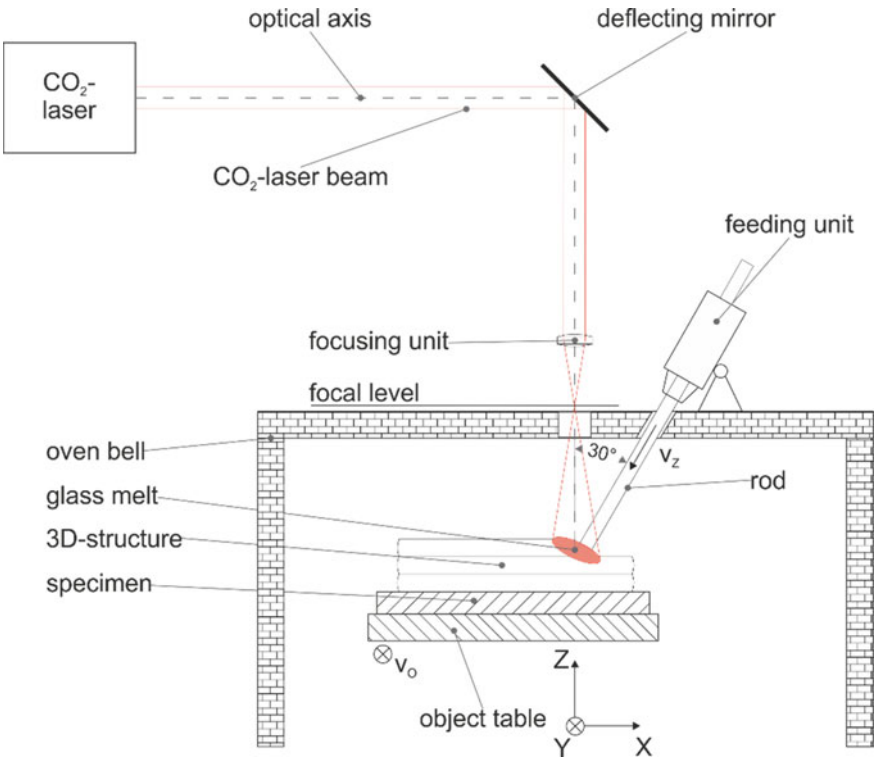


**Fig. 2** Adaptation of the experimental set-up for the Direct Energy Deposition Laser process, replacing the heating plate with a furnace bell

during the experiments.

$$f = \frac{v_Z}{v_O} \tag{2}$$

Experiments conducted with the set-up (Fig. 1) had a constant ratio $f = 1$. The heating unit had an average temperature of 515.5 °C at its surface with a standard deviation of 7 K. In a range with a line energy of 172 J/mm to 202 J/mm, average layer widths of 5.5 mm and layer heights of 2.25 mm could be produced with borosilicate glass. It was observed that with increasing number of layers, the influence of thermal conduction and convection of the heating unit steadily decreases. The resulting thermal gradient during production increased over the height of the additively manufactured structure. This means that there is no heat accumulation in the structure. In a false colour image Fig. 3, the temperature distribution on the glass surface of the structure can be seen qualitatively. The emission coefficient for glass was $\varepsilon = 0.8$ (manufacturer's specification). The temperature curves of the ROI 1 line (Fig. 3) can be seen in Fig. 4. A striking point is the interaction area between

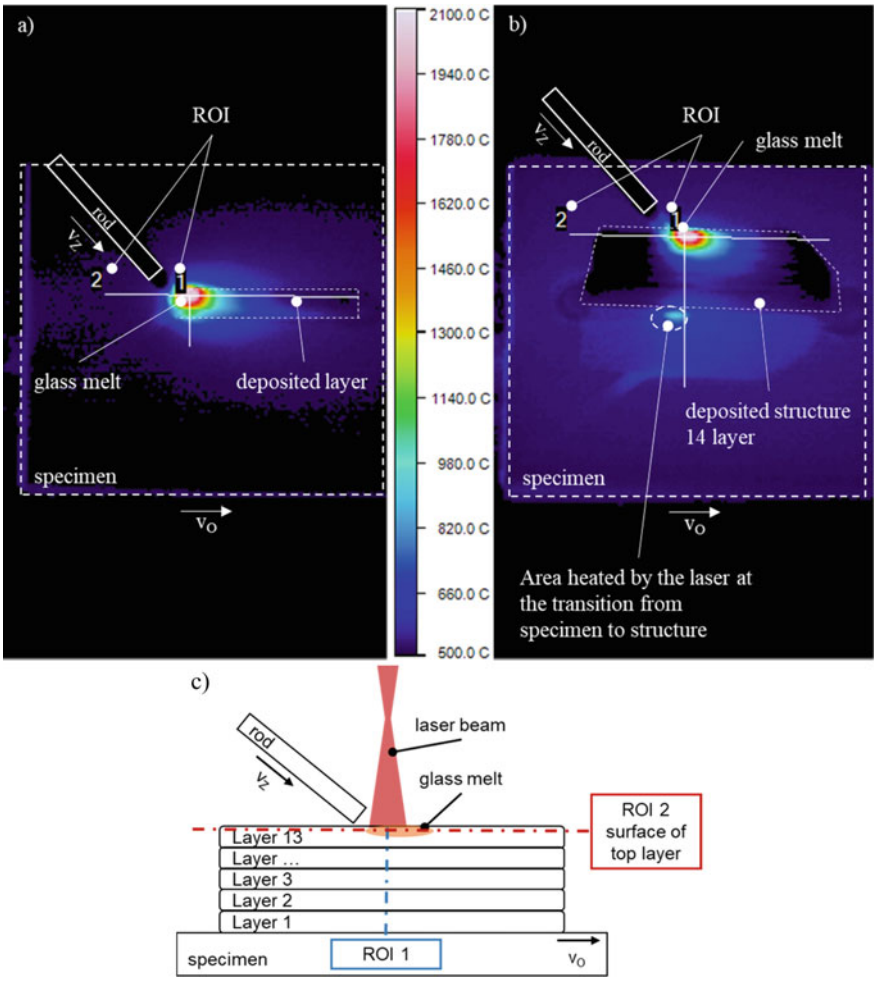


**Fig. 3** False colour image of the temperature distribution on the surface of the sample. The left image **a** shows the process of the first layer. The right picture **b** shows the process during the fourteenth layer. The bottom picutre **c** shows a sketch of the 13 layer structure with ROI 1 and 2. The emission coefficient for glass was set to $\varepsilon = 0.8$ (manufacturer's specification)

the defocused laser and the specimen at the base of the structure. Each layer is exposed to a different thermal load. This leads to the remaining thermal stresses exceeding the stresses that the material can withstand during cooling or renewed abrupt heating. Figures 4 and 5 show that high temperature gradients occur in the additive manufacturing of glass.

Above the glass transition temperature $T_G$ (Duran® $T_G = 525$ °C), it is assumed that glass has a liquid state (Jebsen-Marwedel and Brückner 2011). This explains the compensation of the prevailing temperature gradients around the centre of the glass

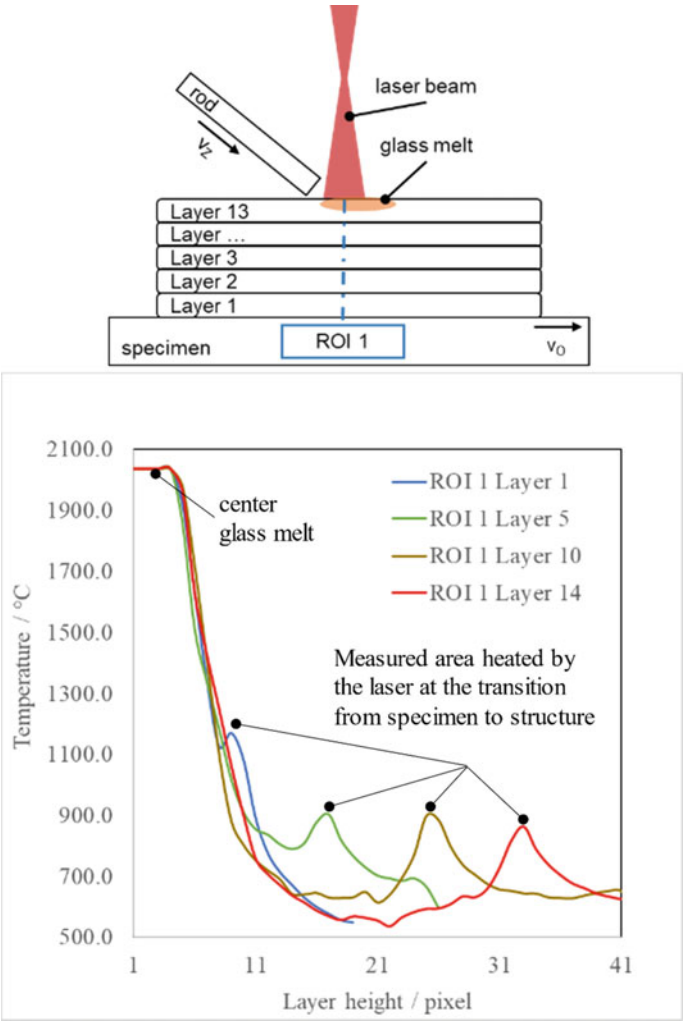


**Fig. 4** The temperature curve is shown as a line profile along the ROI 1 line (Fig. 3). Measured from the centre of the glass melt over the height of the structure. No quantitative value can be assigned on the x-axis to individual pixels due to the inclination and low resolution of the thermal imaging camera

melt. In the edge regions of the structure, visible at the transition from ROI 2 layer 14 at the end of the layer (Fig. 5), the temperature gradient between structure and specimen is approximately 100 K. The further away the layer is from the heating unit, the temperature approaches room temperature and the temperature gradient becomes greater. The prevailing temperature cannot be displayed in Fig. 3 because it is outside the measuring range of the thermal imaging camera. At temperatures below the glass transition temperature $T_G$, it is assumed that glass takes on the behaviour of a solid

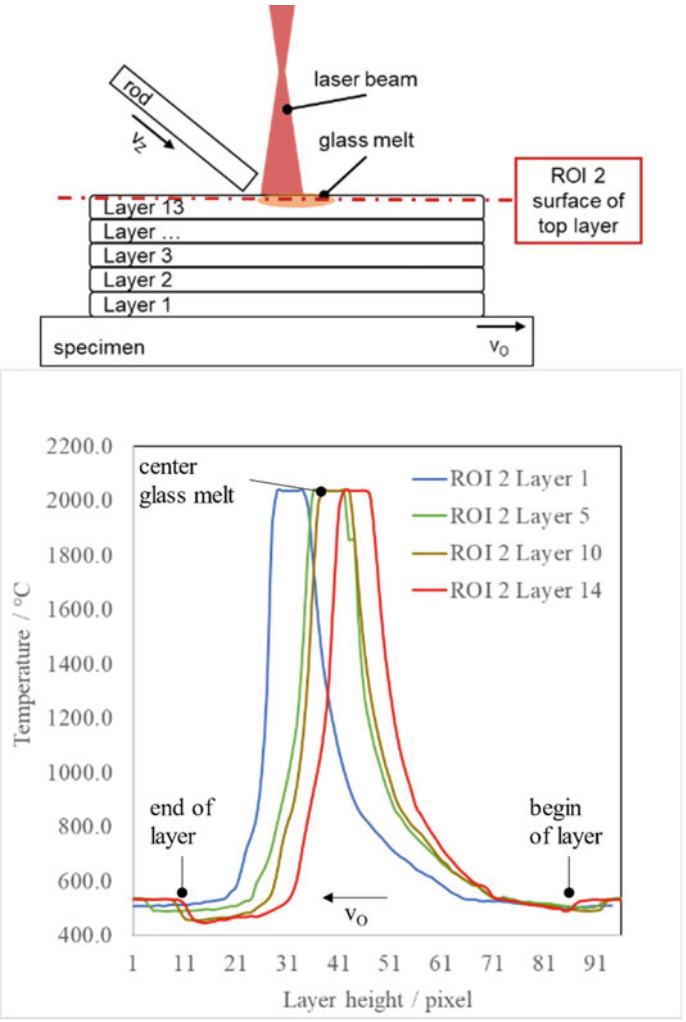


**Fig. 5** The temperature curve is shown as a line profile along the ROI 2 line on the surface of the top layer. Measured from the beginning of a deposited layer to the end of deposited layer on the top of the structure. No quantitative value on the x-axis can be assigned to individual pixels due to the inclination and low resolution of the thermal imaging camera

(Jebsen-Marwedel and Brückner 2011). Thus, the tolerable temperature gradients are much lower and this has been shown during the experimental tests. In our experiments the number of possible layers ran into the limit of about 15 layers, after which the structures broke due to thermal stresses. To manufacture higher structures additively, the experimental setup was modified. The addition of a furnace bell enables a constant ambient temperature (Fig. 2). For the further experiments, the ratio f was changed to f = 1. The laser power could be reduced to P = 79 W with a variance of ± 4 watts. This

corresponds to a line energy of 79 J/mm. With these values, specimens were made with both borosilicate and soda lime glass. Compared to the fabricated structures with the structure in Fig. 1, the structures with the experimental setup in Fig. 2 do not have the waviness of the applied layers similar to the FDM process. The single layers are homogeneously bonded and do not show any notches at the sides. In the transition between sample and structure, an optical separation can be seen. According to Vogel (1993) and Jebsen-Marwedel and Brückner (2011), the optical separation can be a streak in the glass, which is formed due to a viscosity difference. In the further layer structure of the single track wall (Fig. 6) such optical separations are not visible. It can be concluded from this at a homogeneous temperature field and thus a homogeneous viscosity existed. Due to the oven bell, non-contact measurement methods and the temperature prevailing there, contact measurement methods could not be used for temperature measurement. Figure 7 shows a planar application. Here, three layers

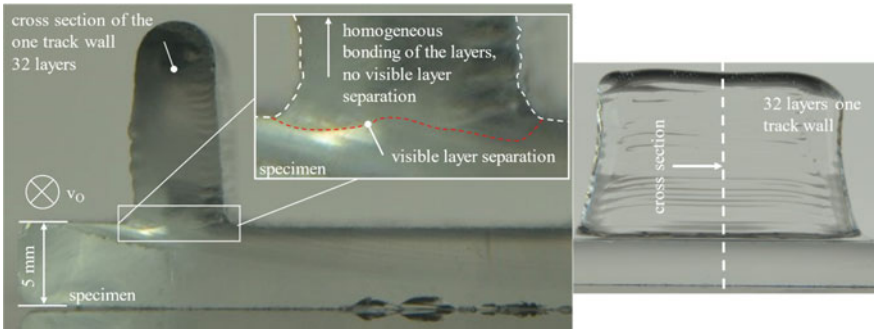


**Fig. 6** Cross-section of a borosilicate glass specimen. An one-track wall with 32 layers i applied to the specimen. There is a visible layer separation at the transition between the specimen and the structure

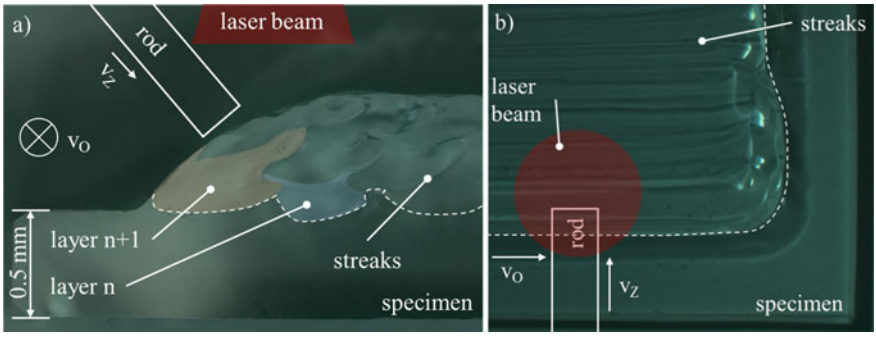


**Fig. 7** Schematically, the DED-L process has been drawn in both figures. **a** Shows the cross-section of (**b**). **b** Shows the top view of the structure. The individual glass streaks can be seen, which are parallel to the direction of additiv manufacutring process. The pictures are taken under a light microscope

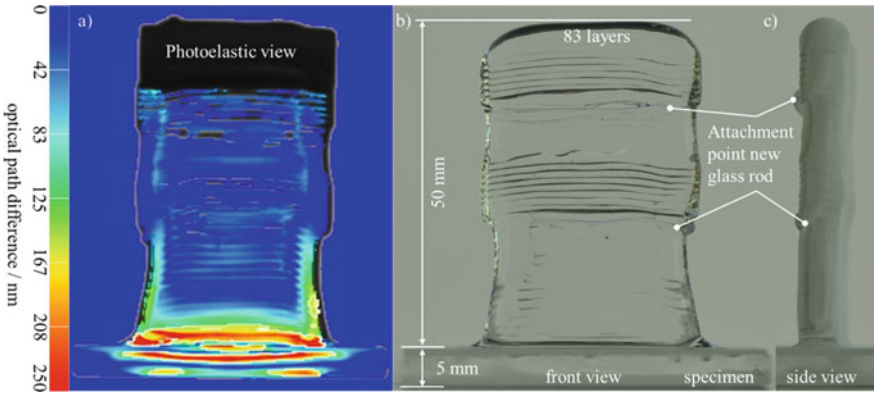


**Fig. 8** Shows a component made of borosilicate glass with 83 layers and a height of 50 mm after thermal post-treatment. On the left in a, the component is examined with the photoelasticity for differences in the optical path difference in order to draw conclusions about stress concentrations. **b** Shows the front view and **c** the side view with the existing final contour

were deposited on the surface. Figure 7a shows the cross-section of Fig. 7b. Figure 7b shows the top view of the structure. The individual glass streaks can be seen, which are parallel to the direction of additive manufacturing process. Figure 7a clearly shows a mixing of the layers. The number and distinctness of the streaks indicate that different temperature conditions prevail when applying a layer to a surface compared to the construction of a single track wall. In order to prevent fracture in the structure during cooling to room temperature and to minimise thermal stresses in the component, it is thermally post-treated. After the manufacturing process, the oven was switched off and the sample cooled down with the oven. The component was then examined for existing stresses using the Strainscope S3/180 device from ilis. The optical path difference was analysed. This shows the sum of existing stresses over the thickness of the component (Fig. 8a). The wavelength of the light is accelerated or slowed down depending on the existing stress in the component. The interference of the outgoing light wave with the measured light wave indicates the optical path difference and allows conclusions to be drawn about the stresses present in the component. The black area in Fig. 8a shows the support, which cannot be penetrated by light. This was necessary to align the component perpendicular to the beam path of the photoelasticity. Figure 8b shows the front view of the manufactured component with 83 layers and a height of 50 mm. Figure 8c shows the component in side view. The attachment points of the new glass rod can be clearly seen in both pictures. In the lower third of the structure, a slightly wavy surface is only visible in the photoelastic view. A concentration of stresses is present at the transition between specimen and structure. Indicated optical path differences in the edge areas or on the wavy surface can also be due to changed reflection or transmission conditions on the curved surface.

## 4 Conclusion

With the extended experimental setup of the DED-L process, we were able to show that the additive manufacturing of individual large-volume glass components is possible compared to the state of the art. The use of glass rods creates a basis that coloured glass rods can also be selectively fed. Furthermore, the processing of quartz (Fröhlich et al. 2020), borosilicate and soda-lime glass has been demonstrated with the experimental setup. Other types of glass, provided they are available as rods, are conceivable with this set-up, as it is possible to adjust to the type of glass by regulating the ambient temperature in the process chamber and adjusting the laser power. The temperature measurements show that the interaction between the laser and the glass creates very high temperature gradients of up to 1500 K on the surface. In order to better distribute the resulting thermal stresses, the entire component must be kept around the glass transition temperature during production. It has been shown that streaking occurs more frequently in the glass when applied to the surface. This may be due to changing thermal boundary conditions compared to a one-track wall. To reduce the formation of streaks, further tests are planned with variation of the temperature in the process chamber, change of the ratio of the interaction area glass and laser in relation to the rod thickness and thermal simulations. The implementation of temperature measurement technology in the extended setup will help to generate more data and understanding of the prevailing temperatures in the process zone. The cooling of the sample with the switching off the furnace has shown that residual stresses are still present in the component.

Investigations with controlled cooling to reduce the stresses to a minimum are planned. A near-net-shape production could be implemented, but a post-processing is still necessary. Particular attention is being paid to the starting points of new glass rods. The waviness in the surface can be compensated by laser polishing.

**Acknowledgements** Part of the investigations were carried out of the project “Production and design methods for the efficient production of individual structures from silicate materials using Wire-Laser Additive Manufacturing (WLAM) -ProGlas3D”. Special thanks go to the company 3D Schilling GmbH, which worked with us on the project. The Thüringer Aufbaubank EFRE (2017FE9085) funds the project. The authors are grateful to LumaSense Technologies GmbH for providing the Mikron thermal imaging camera MC320FHT.

## References

Fateri, M., Gebhardt, A.: Selective laser melting of soda-lime glass powder. Appl. Ceram. **12**(1), 53–61 (2015). https://doi.org/10.1111/ijac.12338

Fateri, M., Gebhardt, A., Thuemmler, S., Thurm, L.: Experimental investigation on selective laser melting of glass. Phys. Procedia **56**, 357–364 (2014). https://doi.org/10.1016/j.phpro.2014.08.118

Fröhlich, F., Hildebrand, J., Bergmann, J.P.: Herstellung individueller Strukturen aus silikatischen Werkstoffen mittels Wire-Laser Additive Manufacturing. In: Glasbau 2020, Ernst, Wilhelm & Sohn, pp. 287–297 (2020)

Gal-Or, E., Gershoni, Y., Scotti, G., Nilsson, S.M., Saarinen, J., Jokinen, V., Strachan, C.J., Boije af Gennäs, G., Yli-Kauhaluoma, J., Kotiaho, T.: Chemical analysis using 3D printed glass microfluidics. Anal. Methods **11**, 1802–1810 (2019). https://doi.org/10.1039/C8AY01934G

Grabe, T., Lammers, M., Wang, S., Wang, X., Rettschlag, K., Sleiman, K., Barroi, A., Biermann, T., Ziebehl, A., Röttger, J., Ley. P.-P., Wolf, A., Jaeschke, P., Hermsdorf, J., Kaierle, S., Ahlers, H., Lachmayer, R.: Additive manufacturing of fused silica using coaxial laser glass deposition: experiment, simulation, and discussion. Laser 3D Manuf. **8**(11677), 45–46 (2021). https://doi.org/10.1117/12.2577205

Gräf, S., Staupendahl, G., Gerling, P., Müller, F.A.: Optical constants n and κ of various technical and optical glasses at $\lambda = 10.59$ μm. J. Appl. Phys. **113**. https://doi.org/10.1063/1.4772619

Jebsen-Marwedel, H., Brückner, R.: Glastechnische Fabrikationsfehler, „Phatologische" Ausnahmezustände des Werkstoffes Glas und ihre Behebung. Eine Brücke Zwischen Wissenschaft, Technologie Und Praxis, Springer, Berlin, Heidelberg. (2011). https://doi.org/10.1007/978-3-642-16433-0

Khmyrov, R.S., Grigoriev, S.N., Okunkova, A.A., Gusarov, A.V.: On the possibility of selective laser melting of quartz glass. Phys. Procedia **56**, 345–356 (2014). https://doi.org/10.1016/j.phpro.2014.08.117

Khmyrov, R.S., Protasov, C.E., Grigoriev, S.N., Gusarov, A.V.: Crack-free selective laser melting of silicia glass: single beads and monolayers on the substrate of the same material. Int. J. Adv. Manuf. Technol. **85**, 1461–1469 (2016). https://doi.org/10.1007/s00170-015-8051-9

Kinzel, E.C., Luo, H., Pan, H.: Additive manufacturing of glass. J. Manuf. Sci. Eng. **136**(6) (2014). https://doi.org/10.1115/1.4028531

Klein, S., Simske, S., Parraman, C., Walters, P., Huson, D., Hoskins, S.: 3D Printing of Transparent Glass. HP Laboratories Technical Report (2012)

Klein, J., Stern, M., Franchin, G., Kayser, M., Inamura, C., Dave, S., Weaver, J.C., Houk, P., Colombo, P., Yang, M., Oxman, N.: Additive manufacturing of optically transparent glass. 3D Print. Additive Manuf. **2**(3) (2016). https://doi.org/10.1089/3dp.2015.0021

Klocke, F., McClung, A., Ader, C.: Direct laser sintering of borosilicate glass. Int. Solid Freeform Fabric. Symp. (2004). https://doi.org/10.26153/tsw/6986

Kotz, F., Plewa, K., Bauer, W., Schneider, N., Keller, N., Nargang, T., Helmer, D., Sachsenheimer, K., Schäfer, M., Worgull, M., Greiner, C., Richter, C., Rapp, B.E.: Liquid glass: a facile soft replication method for structuring glass. Adv. Mater. **28**(23), 4646–4650 (2016). https://doi.org/10.1002/adma.201506089

Kotz, F., Arnold, K., Bauer, W., Schild, D., Keller, N., Sachsenheimer, K., Nargang, T.M., Richter, C., Helmer, D., Rapp, B.E.: Three-dimensional printing of transparent fused silicia glass. Nature **544**, 337–339 (2017). https://doi.org/10.1038/nature22061

Lee, I., Manthriam, A., Marcus, H.L.: Selective laser sintering of alumina-zinc borosilicate glass composites using monoclinic HB02 as a binder. Int. Solid Freeform Fabric. Symp. (1995). http://hdl.handle.net/2152/68689

Liu, C., Qian, B., Ni, R., Liu, X., Qiu, J.: 3D printing of multicolor luminescent glass. Roy. Soc. Chem. Adv. **8**(55), 31564–31567 (2018). https://doi.org/10.1039/C8RA06706F

Luo, J., Gilbert, L.J., Bristow, D.A., Landers, R.G., Goldstein, J.T., Urbas, A.M., Kinzel, E.C.: Additive manufacturing of glass for optical applications. In: Proceedings 9378, Laser 3D Manufacturing III (2016). https://doi.org/10.1117/12.2218137

Luo, J., Gilbert, L.J., Qu, C., Landers, R.G., Bristow, D.A., Kinzel, E.C.: Additive manufacturing of transparent soda-lime glass using a filament-fed process. J. Manuf. Sci. Eng. **136**(6) (2017). https://doi.org/10.1115/1.4035182

Luo, J., Hostetler, J.M., Gilbert, L.J., Goldstein, J.T., Urbas, A.M., Bristow, D.A., Landers, R.G., Kinzel, E.C.: Additive manufacturing of transparent fused quartz. Opt. Eng. **57**(4) (2018). https://doi.org/10.1117/1.OE.57.4.041408

Nguyen, D.T., Meyers, C., Yee, T.D., Dudukovic, N.A., Destina, J.F., Zhu, C., Duoss, E.B., Baumann, T.F., Suratwala, T., Smay, J.E., Dylla-Spears, R.: 3D-printed transparent glass. Adv. Mater. **29**(26) (2017). https://doi.org/10.1002/adma.201701181

Schaeffer, H.A., Langfeld, R.: Werkstoff Glas. Alter Werkstoff Mit Großer Zukunft, Technik Im Fokus. (2020). https://doi.org/10.1007/978-3-662-60260-7

Seel, M., Akerboom, R., Knaack, U., Oechsner, M., Hof, P., Schneider, J.: Additive manufacturing of glass components—exploring the potential of glass connections by fused deposition modeling, challenging glass 6—conference on architectural and structural applications of glass. https://doi.org/10.7480/cgc.6.2161

Vogel, W.: Glasfehler, Springer, Berlin. Heidelberg (1993). https://doi.org/10.1007/978-3-642-58048-2

Witzendorff, P., Pohl, L., Suttmann, O., Heinrich, P., Heinrich, A., Zander, J., Bragard, H., Kaierle, S.: Additive manufacturing of glass: $CO_2$-Laser glass deposition printing. Procedia CIRP **74**, 272–275 (2018). https://doi.org/10.1016/j.procir.2018.08.109